



HAL
open science

Development of the CATHARE 3 three-field model for simulations in large diameter horizontal pipes

Philippe Fillion

► **To cite this version:**

Philippe Fillion. Development of the CATHARE 3 three-field model for simulations in large diameter horizontal pipes. NURETH 2019 - 18th International Topical Meeting on Nuclear Reactor Thermal Hydraulics, Aug 2019, Portland, United States. pp.6271-6282. cea-04382534

HAL Id: cea-04382534

<https://cea.hal.science/cea-04382534>

Submitted on 9 Jan 2024

HAL is a multi-disciplinary open access archive for the deposit and dissemination of scientific research documents, whether they are published or not. The documents may come from teaching and research institutions in France or abroad, or from public or private research centers.

L'archive ouverte pluridisciplinaire **HAL**, est destinée au dépôt et à la diffusion de documents scientifiques de niveau recherche, publiés ou non, émanant des établissements d'enseignement et de recherche français ou étrangers, des laboratoires publics ou privés.

DEVELOPMENT OF THE CATHARE 3 THREE-FIELD MODEL FOR SIMULATIONS IN LARGE DIAMETER HORIZONTAL PIPES

Philippe Fillion

CEA, DEN, STMF, Université Paris-Saclay, F-91191 Gif-sur-Yvette, France
philippe.fillion@cea.fr

ABSTRACT

During hypothetical Loss of coolant accident in a PWR caused by a large break in the primary circuit, the reactor core is uncovered. Emergency core cooling is then activated and the accident enters the reflooding phase. Complex two phase flows and heat transfer phenomena occur during this phase and their analysis request detailed models, included in system codes such as CATHARE.

A three-field model has been previously implemented in CATHARE 3 and applied to reflooding calculations in the core. This paper aims to describe the extension of this three-field model to the primary circuit, especially for hot legs, in order to improve the simulation of liquid droplet transport from the core to the steam generators.

For vertical flows, such as in the core, a comparison of correlations for the entrainment and deposition terms against steam-water data series allowed to select a model for the film-droplets mass exchange. These correlations established for vertical flows are not applicable in horizontal geometries with large diameters such as the hot legs where, during the reflooding phase, the flow regime is dispersed or stratified with entrained droplets. In this case, a specific deposition term based on a model developed from air-water experiments, accounting gravity and turbulent diffusion mechanisms, is used. Dedicated correlations for the entrainment rate and the droplet diameter complete the package of closure laws. These models are assessed against experimental data obtained in horizontal pipes with various diameters and with various inlet gas and liquid superficial velocities.

KEYWORDS

LOCA, hot leg, droplet entrainment, three-field model

1. INTRODUCTION

During Loss of Coolant Accidents (LOCA) in Pressurized Water Reactors (PWR) featuring a large break in the primary circuit, after the first blowdown phase, emergency systems inject large amounts of liquid water into the circuit in order to refill the pressure vessel which has been previously partly emptied. The core is then quite hot and the reflooding phase may take some minutes or more. The boiling two phase flow at low pressure along the rod bundle is quite complex, resulting in small droplet production usually at the quench front. These droplets are carried out by a strong ascending steam flow towards the upper plenum and beyond, to the steam generators, where they vaporize, creating the "steam binding" effect. The droplet behavior out of the core is of great importance for the temperature history of the fuel and cladding and must be predicted as accurately as possible. Moreover, at the beginning of reflooding, strong flow rate oscillations may occur. In horizontal and sloping parts of hot legs, complex flows including stratified water and mist droplet flow have been predicted, sometimes in countercurrent conditions. Usual six-equation models used in system thermohydraulic codes may encounter difficulties in such situations. More advanced three-field

models, sharing the liquid flow in a droplet part and a continuous part, improve the analysis capabilities [1], as far as they can be validated against relevant experiments.

The three-field model of the CATHARE 3 system code [2] features a nine-equation system, three mass balance equations, three momentum equations and three energy balance equations for each of the 3 fields: continuous liquid, liquid droplets and gas phase. This model has been previously developed and assessed for vertical two-phase flows in tubes and rod bundles, especially for dryout prediction [3,4,5,6]. Assessment of a first set of closure laws for the three-field model was done against reflooding separate effect tests (PERICLES and RBHT) and against the reflooding phase of a LBLOCA (Large Break Loss of Coolant Accident) simulated on BETHSY facility [7]. Simulation of the integral test BETHSY 6.7c showed the ability to predict the quench front motion and the clad temperatures in the core. The flow behavior at the outlet of the core is well predicted. However, the authors of the simulation concluded that the behavior of the droplet downstream of the core was not well captured since no adequate closure laws were available for the upper plenum and the hot leg. The conclusion in this previous paper mentioned some lacks in the validation matrix, especially for the upper plenum and hot leg geometries. Separate Effect Tests (SET) experiments, SEROPS-2 and REGARD, will be used respectively for these parts of the primary circuit.

The present paper aims at filling the gap and features new closure laws and validation in a hot leg geometry. Experimental databases in large diameter horizontal pipes, including REGARD, used as Separate Effect Tests for the development of new models and their validation. New closure laws for the entrainment and deposition terms and the droplet diameter dedicated to these conditions are suggested and analyzed.

2. EXPERIMENTAL DATA IN LARGE DIAMETER HORIZONTAL PIPES

Numerous experimental facilities for measurements of entrainment or deposition of droplets in horizontal pipes exist or have been built in the past, e.g. [8,9,10]. The test section usually consists in a long pipe, of several meters or a few tens of meters, with an inner diameter comprise from a few centimeters to 10 cm, exception for a 15.3 cm diameter but inclined pipe reported by Mantilla [10]. The length-to-diameter ratio L/D is roughly comprise between 250 and 500. In most cases, the flow is thus fully developed and the location of the measurements corresponds to equilibrium conditions in term of entrainment and deposition of droplets (i.e. the entrainment rate is equal to the deposition rate). When the diameter of the pipe increases, the vertical stratification of the droplets flow due to the gravity becomes more and more significant. Hot legs of a French PWR have a diameter about 0.7 m and a straight line about 6-7 m length. The L/D ratio is in this case close to 10. Because of the low L/D ratio, the expected flow is not fully developed, and probably has not reached the entrainment/deposition equilibrium and presents a strong stratification of the droplet field.

Dedicated experiments providing data in a scaled-down hot leg geometry exist. This is the case of the MHYRESA facility at CEA-Grenoble, aimed at studying the entrainment of liquid from the upper plenum to the steam generator (SG) inlet chamber, which can occur in case of LOCA or Loss of Heat Removal System (LORHR) during mid-loop operation [11]. Several runs were performed with different air-water flow configuration and geometries with a pipe diameter of 0.118 m and 0.351 m. More recently, effect on the droplet entrainment on the CCFL phenomenon during the reflux condensation mode of a SBLOCA were studied in the COLLIDER test facility [12], consisting of a scaled-down (1/3.9) PWR hot-leg pipe, with a diameter of 190 mm. However, such of experiments have not been investigated in the present paper, focused on the analysis of flows within straight horizontal pipes, leaving aside for the moment the consideration of the bend in the leg.

2.1. REGARD experiments

REGARD experimental program has been designed to overcome some of the lack of data in horizontal pipes, which could be extrapolated in PWR Hot Leg conditions, allowing construction for dedicated models of entrainment or deposition rates [13,14,15]. This air-water experiment features a 24 cm diameter, 4 m long horizontal Plexiglas pipe (see Figure 1).

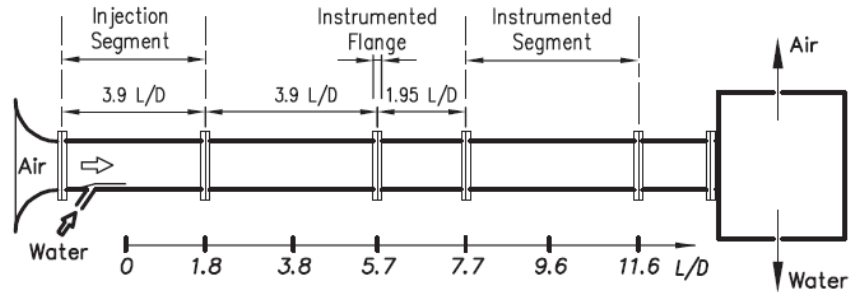


Figure 1. REGARD test section (from [13]).

The entrainment campaign was focused on measurements in wavy-stratified flow conditions. Air and water at near atmospheric pressure and at a temperature equal to 30°C were injected at the inlet of the test section at several volumetric flowrates: four air flowrates of 3100, 3900, 5400 and 6000 Nm³/h (Normalized flowrate corresponding to a volume reduced to 0°C and 1013 hPa), corresponding to superficial velocities J_g of 19.8, 24.8, 38.2 and 38.2 m/s respectively, and two different volumetric flowrates for the water, 3 m³/h and 6 m³/h, corresponding to superficial velocities J_l equal to 0.018 m/s and 0.036 m/s respectively.

Several instrumentation techniques were used for the entrainment campaign. Local measurements of droplet flow rates, diameter and velocities, as well as liquid film thickness and surface wave amplitude and celerity have been performed along the test section. Three laser beams were used to quantify the droplet velocity and droplet diameter (laser granulometry). The uncertainty of the droplet diameter has not been calculated. An isokinetic probe was located just downstream the laser beams and placed at different locations of the cross section for the measurement of the local mass flowrate of droplets. The estimated uncertainty of the droplet mass flowrate is 0.003 g/s. A resistive wire network, called BANJO, was devoted for the measurement of the liquid film (interfacial wave frequency, wave velocity, height ...). The total uncertainties on the liquid level reaches up to $\pm 7.5\%$. The measurements by BANJO and by the laser and the isokinetic probe are available at different locations along the test section. These devices were supplemented by direct visualization of the flow, using a high speed camera.

The analysis of several series of runs allowed to build entrainment rate values in steady flows. The large diameter is closer to the reactor conditions than any other known experiment with detailed measurement.

2.2. Williams experiments

These air-water experiments at near atmospheric pressure, analyzed by Williams et al. [9], were performed in a long horizontal test section (26 m) including a pipe with an inner diameter of 0.0953 m. Local droplet fluxes were measured using a sampling tube. Total entrainment flux was provided in steady state conditions with a large range of water and gas flow rates. Different procedures, discussed in [9], were used to calculate the total entrainment flux. For this quantity, the calculation from the vertical profile of the entrainment flux allows an accuracy within 5%. Local film heights were also measured using a conductance technique, with an accuracy of about 5%. This test series has been retained in CATHARE validation matrix in order to

evaluate the diameter effect for the closure laws. For future simulations of transient tests involving droplet entrainment performed in BETHSY facility, the Williams test section also takes the advantage to have a diameter close to but smaller than the diameter of the horizontal legs of the BETHSY facility, allowing, with REGARD experiment, to frame the BETHSY geometry for this point.

Runs were carried out with different conditions in term of superficial velocities. Air superficial velocities vary from 26 to 88 m/s whereas water superficial velocities are comprise in the range 0.02-0.12 m/s. In these conditions, the flow is stratified for the lowest values of the gas velocities. According to Williams et al. [9], the flow becomes stratified-annular for air superficial velocities and water superficial velocities around 40-50 m/s and 0.03 m/s. For the highest air superficial velocities, 68 m/s and more, asymmetric annular flow is obtained in the pipe. Local film heights and local droplet flux were measured at different location of the pipe, allowing to obtain vertical profiles of the droplet flux and the droplet concentration.

3. CATHARE MODEL

The three-field model of the CATHARE 3 system code is based on a nine-equation system, including mass balance equation, momentum equation and energy balance equation for each of the 3 fields: continuous liquid, liquid droplets and gas phase. Specific correlations dedicated to vertical geometries exist for the entrainment and deposition rates, and for the estimation for the droplet diameter. In this section, we describe the new correlations developed for large diameter horizontal pipes.

3.1. Entrainment model

Pan and Hanratty [16] based their entrainment model in horizontal pipes on the correlation for the entrainment rate developed by several authors in tubes (Dallman et al. [8], Lopez de Bertodano [17]). The correlation reads:

$$m_E = \frac{k'_A V_g^2 (\rho_g \rho_l)^{1/2}}{\sigma} \left(\frac{Q_l}{P_w} - \Gamma_{loE} \right) \quad (1)$$

where ρ_l and ρ_g are the liquid and gas density, σ the surface tension, P_w the perimeter of the pipe and Q_l the film flowrate. The dimensionless atomization constant k'_A is determined from experiments. The critical film flow Γ_{loE} corresponds to the liquid film flowrate per unit length at which the entrainment occurs (oE: onset of entrainment). In the Pan and Hanratty approach, the critical film flow depends on the film velocity around the pipe, which is not constant due to the gravity. This method requires thus the knowledge of the local film around the pipe and has not been retained in the one-dimensional approach of CATHARE, where an averaged critical film flow on the cross section of the pipe is used, simply given by $\Gamma_{loE} = Q_{loE}/P_w$, equivalent to the formulation used in vertical flows.

Pan and Hanratty calculated Q_{loE} from an onset of entrainment Reynolds number:

$$Re_{loE} = 7.3(\log_{10} w)^3 + 44.2(\log_{10} w)^2 - 263 \log_{10} w + 439 \quad (2)$$

Parameter $w = \mu_l/\mu_g \sqrt{(\rho_g/\rho_l)}$, depending on the liquid and gas viscosities μ_l and μ_g , is valid in the range [1.8;28].

Figure 2 shows the model prediction (without CATHARE simulations) against the experimental REGARD data obtained at L/D=3.8. A value of $k'_A = 4 \times 10^{-7}$ is used, close to that proposed by Schimpf et al. ($k'_A = 3.8 \times 10^{-7}$) used in SPACE code [18].

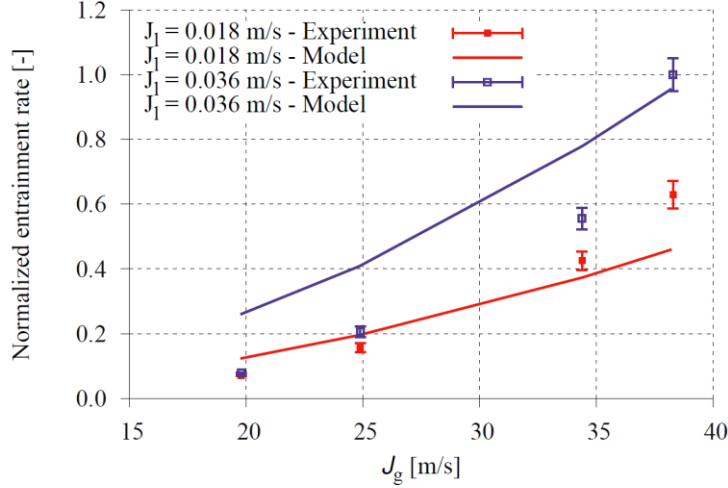


Figure 2. Comparison of the entrainment model with the REGARD data at $L/D=3.8$.

The proposed entrainment model overestimates the experimental entrainment rate for the lowest superficial velocities whereas the entrainment rate tends to be underestimated for the highest gas velocities. For $J_1 = 0.036$ m/s series, the discrepancy between the model the experiment are more important for the lowest gas superficial velocities.

3.2. Deposition model

Neiss [15] developed a one-dimensional deposition model dedicated to large diameter horizontal pipes. In such of geometries, two mechanisms acts on the droplet deposition: gravity and turbulent diffusion. The model suggested by Neiss takes into account these two phenomena, following the works of several authors (e.g. Williams et al. [9]), leading to a deposition rate written as:

$$m_D = kC = (k_{D,grav} + k_{D,diff})C \quad (3)$$

In this equation, C is the concentration of the droplets within the gas core and $k_{D,grav}$ and $k_{D,diff}$ are the deposition velocities relative to the turbulent diffusion and relative to the gravity, respectively.

Following approaches of several authors [9,16], Neiss related the deposition constant to the terminal falling velocity of the droplet:

$$k_{D,grav} = g\tau_p \frac{S_{grav}}{S_{tot}} \quad (4)$$

where τ_p is the relaxation time of the droplet. Neiss suggests a value of τ_p close to 0.1 s, deduced from REGARD experiments, and assumes the deposition due to the gravity only occurs on the lower part of the pipe, so $S_{grav}/S_{tot} = 1/2$. In our model, the variation of the droplet diameter δ is taking account in the calculation of the relaxation time,

$$\tau_p = \frac{1}{18} \frac{\delta^2 \rho_d}{\mu_g} \quad (5)$$

corresponding to a particle following the Stokes regime ($C_D = 24/Re$). In this approach, the relaxation time is calculated from the force balance between the drag and buoyancy forces, and the droplet diameter corresponds to the Sauter mean diameter.

Using the heat transfer / mass transfer analogy, the diffusion turbulent part is modeled by Neiss as

$$k_{D,diff} = 0.023 V_g Re_g^{-0.2} Sc_g^{-2/3} \frac{1}{1 + 2.5 \alpha_d \frac{\rho_d}{\rho_g}} \frac{S_{diff}}{S_{tot}} \quad (6)$$

where Re_g is the gas Reynolds number, Sc_g the Schmidt number, α_d the volumetric droplet fraction, ρ_d the droplet density and S_{diff}/S_{tot} the ratio of the surface where the diffusion turbulent mechanism induced a deposition flux over the total surface of the duct. In the current analysis, the deposition flux is assumed to be identical on the walls of the pipe, so $S_{diff}/S_{tot} = 1$.

In the horizontal pipe with a large diameter, such as in the REGARD experiments, it exists a stratification of the flow. It results a strong concentration of the droplets in the lowest quarter of the pipe. This phenomenon is taken into account by Neiss considering an effective deposition velocity:

$$k_{D,eff} = f_D \cdot k_D \quad (7)$$

where $f_D = 4$.

For REGARD tests, the gravity term is preponderant and contributes roughly to 90-95% to the deposition process. In the case of Williams runs, the contribution diminishes, due to the lowest pipe diameter and higher gas superficial velocities and higher droplet volume fractions.

3.3. Droplet diameter model

The standard correlation of the droplet diameter in CATHARE 3 used in the three-field calculations was obtained by Jayanti and Valette [3] from analysis of high-pressure post-dryout experiments in vertical tubes. For the 6-equation model, the estimation of the maximum droplet diameter takes into account a critical Weber criterion. These correlations significantly overestimate the droplet size obtained during the REGARD entrainment campaign and tests performed in a pipe with the same diameter as for Williams experiments. A short literature review has been achieved in order to find and evaluate correlations for the droplet size in the studied conditions.

Schimpf et al. [18] considered, from an analysis conducted by McCoy and Hanratty, that the volume *median* diameter d_{50} best describes the rate at which droplets deposit into the liquid film at the bottom of a pipe. Schimpf et al. developed of a new correlation of the droplet diameter, including REGARD data, on the work of Al-Sarkhi and Hanratty [19]. These last authors developed correlations of d_{50} and the Sauter mean diameter d_{32} from their own data in a horizontal 0.0254 m diameter pipe and from the Simmons and Hanratty data [20] (diameter 0.0953 m). They provide a simplified expression of d_{32} without dependence against the liquid properties

$$\left(\frac{d_{32} J_g^2 \rho_g}{\sigma} \right)^{0.55} \left(\frac{d_{32}}{D} \right)^{0.36} = 0.154 \quad (8)$$

The expression of the relaxation time, related to the droplet terminal velocity, appearing in the deposition model following the Neiss' approach was obtained from the balance of the buoyancy force and the drag force. The Sauter mean diameter is used as the droplet size in this approach. This diameter is also used for in the expression of the gas-droplet interfacial friction used in the code.

In a review of droplet entrainment in annular flow, Berna et al. [21] propose a correlation of the volume *mean* droplet diameter d_{vm} in horizontal pipes, from the analysis of three databases with various pipe diameters but smaller than REGARD one, from 0.0254 m to 0.0953 m. The database with the largest pipe diameter is that published by Simmons and Hanratty [20], and was obtained on the same test section used

by Williams et al. [9], The correlation obtained by Berna et al. for the mean volume diameter d_{vm} depends on the pipe diameter D and is expressed as a function of the gas and film Reynolds numbers and the gas Weber number based on the pipe diameter as the scale length:

$$\frac{d_{vm}}{D} = 2.634 We_g^{-0.23} Re_g^{-0.54} Re_l^{0.13} \quad (9)$$

To avoid the dependence against the film properties, and because this dependence is weak, the volume mean diameter d_{vm} has been expressed in CATHARE from the gas properties only. In the present CATHARE calculations, a simplified correlation derived from the correlation suggested by Berna et al. is used:

$$d_{vm} = 11.33 We_g^{-0.23} Re_g^{-0.54} D^{1.13} \quad (10)$$

Finally, from the data obtained by Al-Sarkhi and Hanratty, and Simmons and Hanratty, we correlated the Sauter mean diameter from the mean volume diameter with the simple relation

$$d_{32} = 0.60 d_{vm} \quad (11)$$

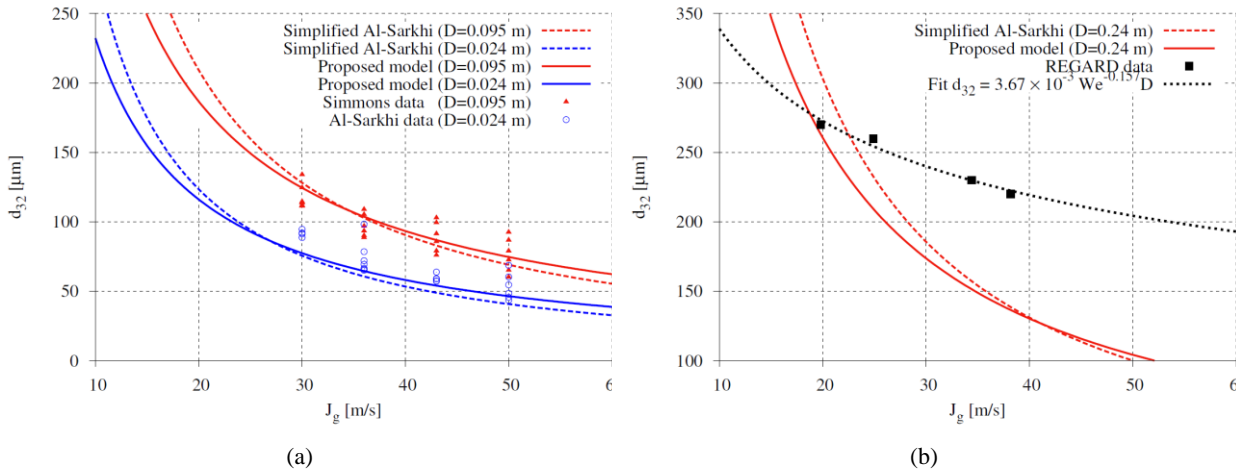


Figure 3. Comparison of the predicted mean Sauter diameter using the simplified Al-Sharki model and the proposed model against experimental data.

The experimental droplet diameters are reasonably predicted in case of the Al-Sarkhi and Hanratty, and Simmons and Hanratty data (Figure 3a) by the proposed model (equations (10)-(11)) and the simplified Al-Sharki model (equation (8)). Both model have the same trends, but the error between the correlation and the experiment is slightly reduced using the proposed model. However, both models do not fit the REGARD experimental values (Figure 3b). One of this reason of these discrepancy is due to the fact that in REGARD, the measured droplet distributions according to their diameter is completely different to those provided by Simmons and Hanratty (see Figure 4).

In Valette and Henry [13], the analysis of the droplet diameter spectrum points out, apart of the pipe diameter effect, that the droplet diameter data produced by Simmons and Hanratty, and Al-Sharki and Hanratty are obtained at the centre line (or at 3/4" above and below the centre line) of these experiments whereas the REGARD data are obtained using the laser measurement system in the lower quadrant of the pipe cross-section. Literature correlations for volume median diameter, such as Tatterson or Kataoka ones, do not predict the REGARD experimental results. From this assessment, the analysis also suggests that "to the fact that in REGARD a considerable number of small droplets disappeared by vaporization in contact to the air. As the number of vaporized droplet is less sensitive to the air velocity than the increase of created

droplet, the volume median diameter is more affected by the loss of its smaller droplets at low air velocity than at high air velocity.” Schimpf et al. observed that the volume median diameters obtained in REGARD show an inverse trend with increasing gas velocity, comparing to those of Simmons and Hanratty, and Al-Sharki and Hanratty. We also remark that the REGARD tests were performed with low droplet volume fraction ($< 0.6 \times 10^{-4}$ for the considered droplet diameter data) instead of a range $2 \times 10^{-4} - 11 \times 10^{-4}$ for the other databases. For a dilute droplet population, the coalescence or breakup of the droplet phenomena affecting the droplet distribution are less sensitive.

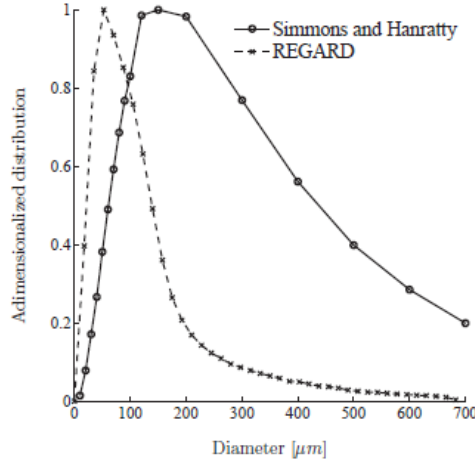


Figure 4. Comparison of the droplet diameter distributions from Simmons and Hanratty and REGARD (figure extracted from [13]).

According to these remarks, it seems to be difficult to correlate the droplet diameter from these three experiments without at least to reanalyze the REGARD databank. Nevertheless, REGARD experimental data for the Sauter mean diameter provided in [13] have the same trend (decrease of the diameter with increasing gas superficial velocity) to those obtained on the two other considered experiments (see Figures 3a and 3b). So, our current study, we first preferred to use a specific correlation fitted on REGARD data for the space-average Sauter mean diameter in the CATHARE simulations of this experiment:

$$d_{32} = 3.67 \times 10^{-3} We_g^{-0.157} D \quad (12)$$

This specific correlation can only be used for the assessment for the entrainment and deposition models against REGARD data, whereas the correlation (10)-(11) can be used in a larger domain, including Williams experiment.

4. CATHARE RESULTS

4.1. REGARD experiments

Figures 5 and 6 show a comparison between the calculated droplet flowrate function of the gas superficial velocity using the Neiss model, the Pan-Hanratty model, the droplet diameter calculated from (12), implemented in CATHARE, and the REGARD experiments with an inlet water volumetric flowrate $Q_l = 3 \text{ m}^3/\text{h}$ and $Q_l = 6 \text{ m}^3/\text{h}$. The droplet flowrate has been normalized by the maximum experimental flowrate obtained for each series. CATHARE well reproduces the increasing of the droplet flowrate at the beginning of the test section. In general, a good prediction of the droplet flowrate profiles along the test section is found, except for the couple ($Q_l = 6 \text{ m}^3/\text{h}$, $J_g = 34.6 \text{ m/s}$), and the code tends to underestimate the experimental values for the highest gas superficial velocities for $Q_l = 3 \text{ m}^3/\text{h}$.

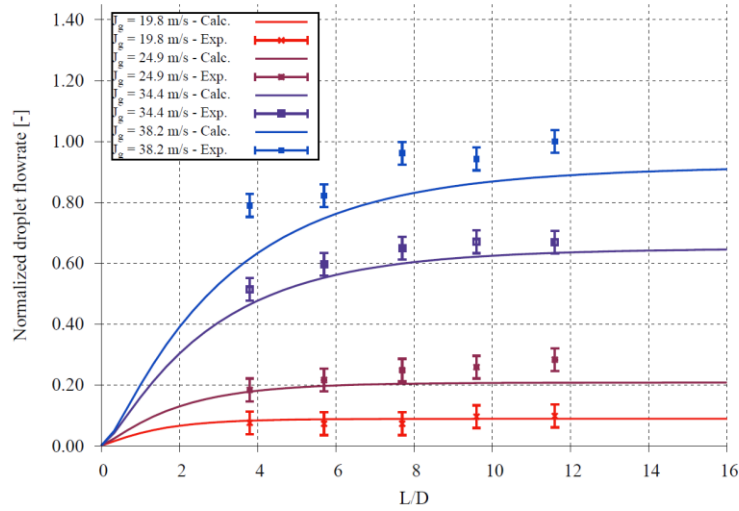


Figure 5. Comparisons of the REGARD experimental droplet flowrates profiles along the test section and the CATHARE simulations for $Q_l = 3 \text{ m}^3/\text{h}$.

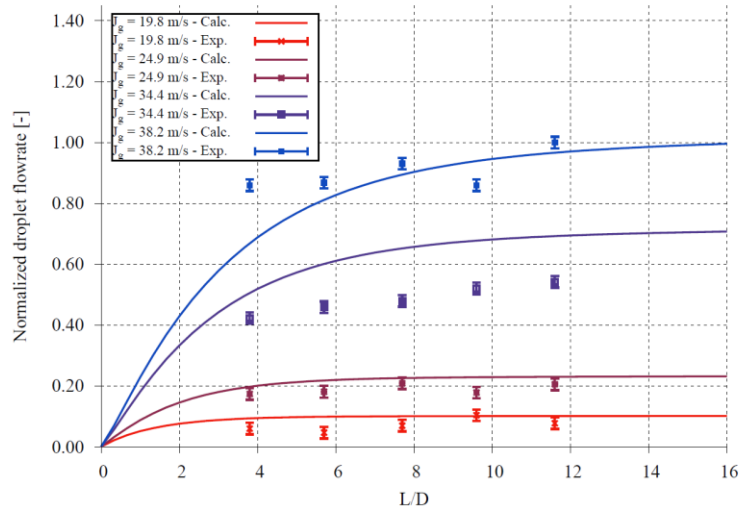


Figure 6. Comparisons of the REGARD experimental droplet flowrates profiles along the test section and the CATHARE simulations for $Q_l = 6 \text{ m}^3/\text{h}$.

4.2. Williams experiments

Figure 7 shows the comparison of the calculated entrainment fraction E (ratio of droplet mass flowrate to total liquid mass flowrate) using the Neiss model, the Pan-Hanratty model with the same value as for the REGARD experiments for the atomization constant, and the droplet diameter calculated from the correlation (10)-(11), against the experimental values obtained by Williams. Simulation agrees with the experimental entrainment fraction with a relative mean absolute error of 23%. The tests with the two lowest gas superficial velocities series are well predicted. The entrainment fraction is underestimated for the intermediate gas superficial velocities tests ($J_g = 37 \text{ m/s}$ and $J_g = 45 \text{ m/s}$), at low liquid velocities. The agreement tends to be better when the liquid velocity increases. The entrainment fraction for $J_g = 68 \text{ m/s}$ and $J_g = 88 \text{ m/s}$, where the flow becomes annular, is rather well predicted, despite of an deposition model more dedicated to wavy-stratified flows, and thus not well adapted for this flow regime.

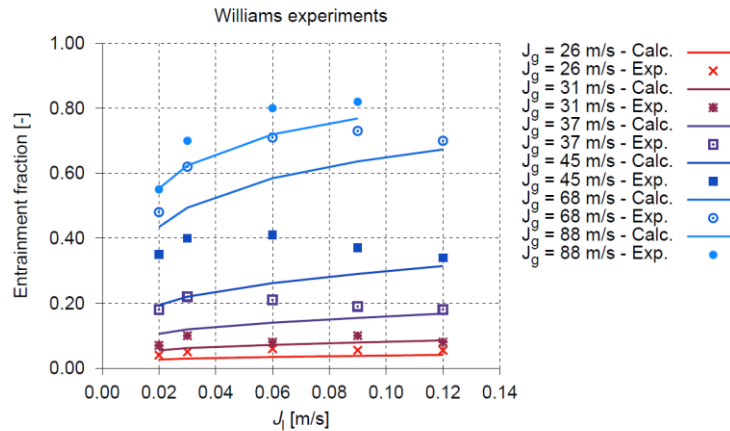


Figure 7. Comparisons of the Williams experimental entrainment fraction E and the CATHARE simulations using an atomization constant $k'_A=4\times 10^{-7}$.

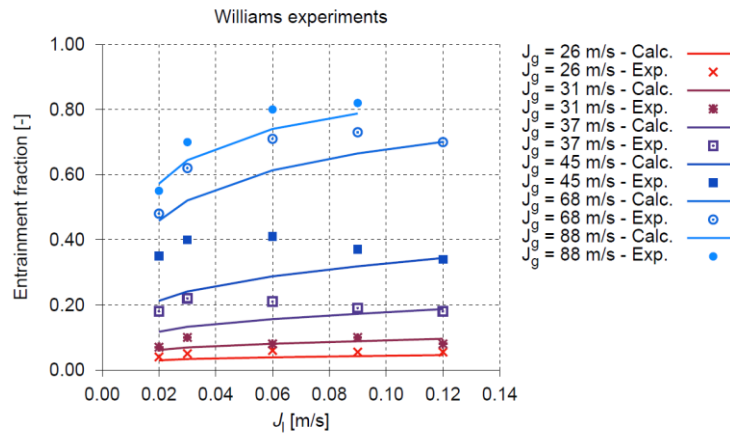


Figure 8. Comparisons of the Williams experimental entrainment fraction E and the CATHARE simulations using an atomization constant $k'_A=4.5\times 10^{-7}$.

The value of the atomization constant $k'_A=4\times 10^{-7}$ is obtained from the analysis of the REGARD tests. However, the experimental entrainment rates used to determine this value do not correspond to equilibrium conditions and are underestimated. Consequently, the atomization constant for the Williams experiments, in fully developed conditions, is probably underestimated. Calculations were thus performed with a higher value of the atomization constant $k'_A=4.5\times 10^{-7}$, which gives better results (Figure 8) with a relative mean absolute error of 17.7% on the entrainment fraction. If the results for the REGARD tests are slightly degraded consequently, the global error on the entire database diminishes.

5. CONCLUSIONS

This work aimed at addressing the assessment of the three-field model of the system code CATHARE 3 against large diameter horizontal pipes, in wavy-stratified and asymmetric annular flow conditions with entrained droplets. This first step of assessment gave encouraging results. Correlations due to Pan-Hanratty

and Neiss, with proposed corrections or modifications for the modeling of the entrainment and deposition of the droplets were assessed against REGARD entrainment and Williams databases.

CATHARE well reproduces the increasing of the droplet flowrate at the beginning of the REGARD test section. Pan-Hanratty model with an atomization constant $k'_A=4.5\times 10^{-7}$ can be used both in REGARD and Williams conditions, and allows, with the suggested models for the deposition term and the droplet diameter, to reproduce experimental data of Williams with a relative mean absolute error of 17.7% on the entrainment fraction.

This new set of correlations included into CATHARE 3 could be improved by the deposition term due the gravitational settling, by a better modeling of the relaxation time of the droplet. In particular, the current model requires a correlation of the droplet size covering various large pipe diameters and flow conditions. Further analysis of the raw data of REGARD for the droplet size distributions will probably give information for the improvement of this correlation. The effective factor introduced by Neiss, allowing to take into account the vertical stratification of the droplets within the pipe, could also be improved from REGARD data or other experiments, considering the experimental vertical profiles of the droplet concentration at different locations and different gas superficial velocities.

ACKNOWLEDGMENTS

CATHARE-3 is developed in the framework of the NEPTUNE project, financially supported by CEA, EDF, Framatome and IRSN.

REFERENCES

1. D. Bestion and G. Serre, "On the modelling of phase-flow in horizontal legs of a PWR," *Nuclear Engineering and Technology*, **44**(8), pp. 871–888 (2012).
2. P. Emonot, A. Souyri, J.L. Gandrille and F. Barré, "CATHARE-3: A new system code for thermal-hydraulics in the context of the NEPTUNE project," *Nuclear Engineering and Design*, **241**(11), pp. 4476–4481, (2011).
3. S. Jayanti and M. Valette, "Prediction of dryout and post-dryout heat transfer at high pressures using a one-dimensional three-fluid model", *International Journal of Heat and Mass Transfer*, **47**, pp. 4895–4910 (2004).
4. S. Jayanti and M. Valette, "Calculation of dry out and post-dry out heat transfer in rod bundles using a three field model", *International Journal of Heat and Mass Transfer*, **48**, pp. 1825–1839 (2005).
5. M. Spirzewski, P. Fillion and M. Valette, "Prediction of annular flows in vertical pipes with new correlations for the CATHARE 3 three-field model, *Proceedings of NURETH-17*, Xi'an, China, (2017).
6. M. Spirzewski and H. Anglart, "An improved phenomenological model of annular two-phase flow with high accuracy dryout prediction capability", *Nuclear Engineering and Design*, **331**, pp. 176–185, (2018).
7. M. Valette, J. Pouvreau, D. Bestion and P. Emonot, "Revisiting large break LOCA with the CATHARE-3 three-field model", *Nuclear Engineering and Design*, **241**, pp. 4487–4496 (2011).
8. J. Dallman, J.E. Laurinat, and T.J. Hanratty, "Entrainment for horizontal annular gas-liquid flow," *International Journal of Multiphase Flows*, **10**(6) pp. 677–690 (1984).
9. L.R. Williams, L.A. Dykhno, and T.J. Hanratty, "Droplet flux distributions and entrainment in horizontal gas-liquid flows," *International Journal of Multiphase Flows*, **22**(1), pp. 1–18 (1996).
10. I. Mantilla, "Mechanistic modeling of liquid entrainment in gas in horizontal pipes," PhD thesis, University of Tulsa, USA (2008).

11. G. Geffraye, S. Laroche, B. Faydide, and G. Ratel, "Analysis of the MHYRESA hot leg entrainment tests," *Proceedings of the 8th International Conference on Nuclear Engineering*, Baltimore, MD, USA, April 2–8 (2000).
12. S. Al Issa and R. Macian-Juan, "Droplets entrainment ratio in a PWR hot-leg pipe geometry," *Nuclear Engineering and Design*, **330**, pp. 1–13, (2018).
13. M. Valette and F. Henry, "Droplet entrainment over a stratified flow in a PWR hot leg: results of the REGARD experiment," Technical Report STMF/LMES/NT/14-046, CEA (2015).
14. F. Henry, M. Valette, and Y. Bartosiewicz, "A model for droplet entrainment rate in horizontal stratified flow," *Proceedings of NURETH-14*, Toronto, Canada (2011).
15. C. Neiss, "Modélisation et simulation de la dispersion turbulente et du dépôt de gouttes dans un canal horizontal," PhD thesis, Université de Grenoble, France (2013) [in French]
16. L. Pan and T.J. Hanratty, "Correlation of entrainment for annular flow in horizontal pipes," *International Journal of Multiphase Flows*, **28**, pp. 385–408 (2002).
17. M. A. Lopez de Bertodano, A. Assad, and S. Beus, "Entrainment rate of droplets in the ripple annular regime for small vertical ducts," *Nuclear Science and Engineering*, **129**(1), pp. 72–80 (1998).
18. J. K. Schimpf, K. D. Kim, J. Heo and B. J. Kim, "Development of droplet entrainment and deposition models for horizontal flow," *Nuclear Engineering and Design*, **50**, pp. 379–388 (2018).
19. A. Al-Sarkhi, T. Hanratty, "Effect of pipe diameter on the drop size in a horizontal annular gas-liquid flow," *International Journal of Multiphase Flows*, **28**(10), pp. 1617–1629 (2002).
20. M.J.H. Simmons and T.J. Hanratty, "Droplet size measurements in horizontal annular gas-liquid flow," *International Journal of Multiphase Flow*, **27**, pp. 861–883 (2001).
21. C. Berna, A. Escrivá, and L.E. Herranz, "Review of droplet entrainment in annular flow: Interfacial waves and onset of entrainment," *Progress in Nuclear Energy*, **74**, pp. 14–43 (2014).